Normal and umklapp phonon decay rates due to phonon-phonon and electron-phonon scattering in potassium at low temperatures

R. C. Albers*
Laboratory of Atomic and Solid State Physics, Cornell University, Ithaca, New York 14853

L. Bohlin†
Department of Physics, University of Nigeria, Nsukka, Nigeria

M. Roy*
Indian Institute of Geomagnetism, Bombay-5, India

J. W. Wilkins*‡
Nordita, Blegdamsvej 17, DK-2100, Copenhagen Ø, Denmark
(Received 23 December 1974)

Phonon decay rates in potassium due to phonon-phonon and electron-phonon scattering are calculated and compared for small wave numbers at low temperatures (~ 1 to 10 K). We find that the phonon-phonon half-widths Γ_{pp} have a strong dependence on the temperature and *magnitude* of $\vec{q}$, but are roughly independent of the *direction* of $\vec{q}$. The electron-phonon half-widths Γ_{ep} are temperature independent, vary slowly with q (linear in q for $q \lesssim 0.3 \times 2\pi/a$), and have a strong directional dependence on $\vec{q}$ for the transverse phonon modes. The umklapp contribution Γ_{pp}^{U} to the total phonon-phonon decay rate $\Gamma_{pp}^{\mathrm{TOT}}$ is also calculated for small q and is shown to have a pronounced temperature dependence whereby $\Gamma_{pp}^{U}/\Gamma_{pp}^{\mathrm{TOT}}$ decreases rapidly at lower temperatures. In comparing the various half-widths we find that at high temperature ($\gtrsim 30$ K) Γ_{pp} dominates Γ_{ep}. At lower temperatures the two are comparable to each other and the situation is complex. Along certain directions in $\vec{q}$ space for certain branches Γ_{ep} may dominate whereas along symmetry directions at small q for the transverse branches Γ_{ep} is zero and Γ_{pp} dominates. The relevance of these and other results are discussed in the context of low-temperature transport properties. Finally we briefly compare our results for potassium with those for two other simple metals, rubidium and aluminum.

I. INTRODUCTION

This paper presents the first estimates of the phonon-phonon scattering rates which are appropriate to low-temperature transport processes in metals. The existing calculations for the metals potassium, rubidium, and aluminum are all directed towards calculating the widths of phonons seen in neutron scattering and are thus inappropriate for transport properties in that (i) the calculations are done for higher temperatures and for larger wave vectors than are desired, and (ii) the calculations do not separate the contributions of normal and umklapp scattering. This second point is crucial for understanding transport properties and will be discussed in detail in Sec. IB and the end of Sec. IV.

In this paper we attempt to partially remedy this lack of information by presenting results of computations on the decay rates of phonons in potassium at a few degrees kelvin of both phonon-phonon (Sec. II) and electron-phonon (Sec. III) scattering, both of which, as we discuss below, are important for understanding low-temperature transport properties. We use the words "partial remedy" because our present calculations are not as accurate as we would like, particularly in the most interesting region of low temperature and small wave vector. The difficulties of extending the present methods of calculations to these regions are extensively discussed in Appendix A.

Our purposes in presenting this paper are (i) to provide some reasonable numbers as a guide for calculations of transport properties at low temperatures; (ii) to stimulate further calculations of phonon-phonon scattering rates in the low-temperature, small-wave-vector region by showing the need for such calculations, presenting the current state of the art in this area, and suggesting where improvements are necessary; and (iii) to detail the interesting and unexpected results we have found (Sec. IV) which we hope will engender some discussion and thought among those interested in the physics of phonons and transport processes.

Before presenting the results of our calculations, we first discuss the relevance they have for transport properties. In particular, in this section we will now develop an increasingly more sophisticated view of how momentum is transferred between the electron and phonon systems in a metal.

A. Two limiting cases

Suppose that momentum is pumped at a constant rate into the electrons by an applied electric field (which has no effect on the ions). A steady-state

distribution of the *electrons*, in which the average momentum is nonzero, is then achieved by various scattering mechanisms of which we shall, in order to state the problem concisely, consider only one-electron-phonon scattering. Momentum transferred to the phonon system by this scattering mechanism can be "redistributed" in two ways: (i) It can be distributed to the other phonons by (anharmonic) phonon-phonon scattering with a characteristic rate Γ_{pp}, or (ii) it can be returned to the electron system by the inverse of the original process, electron-phonon scattering, according to the rate Γ_{ep}.

Clearly there are two limiting cases depending on which rate, Γ_{pp} or Γ_{ep}, dominates. If $\Gamma_{pp} \gg \Gamma_{ep}$, it may be that the phonons drop out of the problem except as a sink for momentum. Then the calculation of transport properties is relatively straightforward. On the other hand, if $\Gamma_{pp} \ll \Gamma_{ep}$, the internal dynamics of the phonon system may play an important role in transport properties.

This latter limit which occurs at low temperatures raises an important question: How does a metal reach internal equilibrium at low temperatures? The question was stated most forcefully by Peierls, [1] for the alkali metals. For these the Fermi surface does not touch the Brillouin zone. Hence, as it turns out, none of the momentum (supplied by the applied electric field) can be dissipated in the process of transferring the momentum to the phonon system. Furthermore the phonon system by itself does not contribute either to momentum dissipation since its internal scattering rates are so small. How then does the system reach equilibrium, or would careful measurements reveal nonlinear dependences on the applied field? We do not answer this question but show that any answer must take into account greater complexities than previously considered. Let us turn now to the two limiting cases for phonon scattering.

1. *Bloch limit* $\Gamma_{pp} \gg \Gamma_{ep}$

For phonons it is simple to show that Γ_{ep} is nearly independent of temperature while Γ_{pp} is a rapidly increasing function of the temperature. [2] Accordingly one might expect that at reasonably high temperatures $\Gamma_{pp} \gg \Gamma_{ep}$. Furthermore there is a subcategory of Γ_{pp}, called umklapp phonon-phonon scattering, Γ_{pp}^{U}, in which the phonon momentum is relaxed to the lattice. So not only is any momentum quickly equilibrated among the phonons but it is rapidly (how rapidly depends on the temperature among other things) dissipated to the lattice. Accordingly we may suppose the phonons to be in an equilibrium state appropriate to *no* electric field being applied, i.e., a state which has no net momentum associated with it. This limiting case was first discussed by Bloch, [3] who showed that the resulting electrical resistivity was linear in temperature at high temperature and went as T^5 at low temperatures. The upper limit is well justified experimentally (after one makes suitable adjustments for the temperature dependences of the phonon frequencies), but the low-temperature limit is in some dispute, especially since we have just pointed out that Γ_{pp} falls rapidly for decreasing temperature.

2. *Phonon-drag limit,* $\Gamma_{pp} < \Gamma_{ep}$

To consider an extreme case, let us suppose that we are at such a low temperature, that phonons have difficulty in equilibrating any momentum that is pumped into them from the electrons (being accelerated by the electric field). Further let us keep in mind that at these temperatures the umklapp phonon-phonon scattering rate Γ_{pp}^{U} is much less than the total phonon scattering rate Γ_{pp}; the former falling exponentially with $1/T$. That being the case, the phonons can only feed momentum back into the electrons—specifically, to the local distribution which is drifting under the influence of the electric field. In steady state the phonon gas has the same drift velocity as the electron gas; we say that the phonons are *dragged* by the electrons. In that phonon-drag regime, i.e., the one in which there is no way to dissipate the momentum, the electrical resistivity goes to *zero*. Of course, in any real sample that situation would not be reached since other momentum absorptive centers—impurities, dislocations, surfaces, etc.—would eventually dominate the low-temperature resistance. Nonetheless, it is clear that there are two distinct limiting cases, and it would be interesting to know which is appropriate as the temperature is lowered.

Before we turn to a discussion of some of the subtleties involved, we should point out why the situation is so special for some alkali metals. Because the Fermi surface does not touch the first Brillouin zone, one very effective method for relaxing electron momentum is not available, that of umklapp electron-phonon scattering which enables some of the momentum to be lost to the lattice in the process of electron-phonon scattering. Accordingly, the considerations discussed above at such great length come into play.

3. *Effect of two limiting cases on electrical resistivity*

It is perhaps worthwhile to point out several features that arise in calculating the electrical resistivity in the two limits. In Fig. 1 the calculated resistivities [4,5] are plotted in units of T^5 for low temperatures (1–10 K). On the Bloch curve the "bump" in the T^5 coefficient is due to the rapid onset of umklapp electron-phonon scattering (in the electron system). At still higher temperatures that coefficient drops, indicating the transition to the linear temperature dependence.

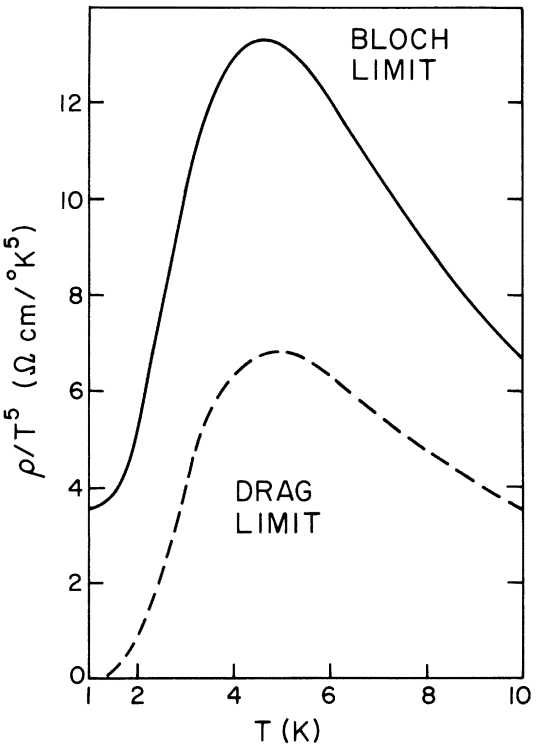

FIG. 1. Calculated temperature dependence of the electrical resistivity in both the Bloch ($\Gamma_{pp} \gg \Gamma_{ep}$) and "phonon-drag" ($\Gamma_{pp} \ll \Gamma_{ep}$) limits. Results for the resistivity divided by the fifth power of the temperature are shown between 1 and 10 K as a solid curve for the Bloch limit and a dashed curve for the phonon-drag limit. In the latter case ρ/T^5 is not strictly zero for $T \lesssim 1.4$ K but rather is many orders of magnitude too small to show up on the figure.

On the other hand, the "phonon-drag-limit" resistivity at low temperatures approaches zero more rapidly than T^5. At high temperatures the drag limit approaches a fixed ratio of the Bloch limit. This results from the incorrect assumption that $\Gamma_{pp} \ll \Gamma_{ep}$ at *all* temperatures and wave vectors. A correct calculation for the resistivity would involve using the appropriate phonon decay rates so that the resistivity "switches" from the drag to the Bloch limit. Clearly this switch in potassium occurs at an experimentally accessible region and any sensible calculation must include this effect. What seems likely as a result of the calculations in this paper is that the details of the switch may be complicated owing to the fact that Γ_{pp} exceeds Γ_{ep} at different temperatures for different phonon polarizations and wave vectors.

B. Normal and umklapp phonon-phonon scattering

The existing calculations of the phonon-phonon scattering rates for the metals potassium,[6] rubidium,[7,8] and aluminum,[9,10] are all directed toward calculating the widths of phonons seen in neutron scattering. As mentioned earlier, these results are inappropriate for our purposes in two ways: (i) All the calculations are for higher temperatures (the lowest being 9 K in potassium) and for higher wave vectors than we desire. As we shall point out, principally in Appendix A, calculations in the desired range put considerable strain on the computing facilities available to us. (ii) The calculations do not separate the contributions of normal and umklapp scattering. This second point deserves some extended discussion.

The Boltzmann equation for phonon distribution $n(\vec{q})$ provides a convenient basis for discussions. Conventionally we may write

$$\frac{Dn(\vec{q})}{Dt} = I(n(\vec{q})), \tag{1.1}$$

where the operator on the left-hand side is the drift operator and on the right-hand side is the collision integral. For simplicity we suppress the possibility of electron-phonon scattering processes discussed in Sec. IA. Formally one can divide $I(n(\vec{q}))$ into two kinds of processes: *normal* ones in which the total momentum of the phonon gas is conserved and *umklapp* ones in which momentum is transferred to (or from) the lattice. To date, no one has solved (1.1) keeping the full structure of the collision integral. The most common approach has been to make relaxation-time approximations for the two kinds of processes. We adopt this procedure in order to discuss the general structure of our results, not knowing of a better approach.

1. Normal processes

Since normal processes conserve the total momentum of the phonon gas, one must allow for the possibility that the scattered phonons relax to some distribution which is drifting with a velocity $\vec{v}$:

$$n_{\text{drift}}(\vec{q}, \lambda; \vec{v}) = [e^{\beta[\hbar\omega_\lambda(\vec{q}) - \vec{q}\cdot\vec{v}]} - 1]^{-1} \tag{1.2}$$

of the phonons. Such a distribution could be set up by the injection of momentum from the electron system as would occur if there were a significant amount of phonon drag. In this case the appropriate relaxation-time approximation is

$$I^N(n(\vec{q}, \lambda)) = -[n(\vec{q}, \lambda) - n_{\text{drift}}(\vec{q}, \lambda; \vec{v})](2\Gamma^N_{pp}). \tag{1.3}$$

In principle, Γ^N_{pp} is a function of wave vector $\vec{q}$, polarization λ, and temperature T [$= (k_B\beta)^{-1}$]. In practice, all the calculations for which Γ_{pp} and Γ^U_{pp} have been separately calculated have usually been restricted to extracting an average Γ_{pp} depending only on temperature. We are, of course, able to

compute (albeit sometimes with dubious accuracy) the full wave-vector and polarization dependence of Γ_{pp}. The difficulty arises in using this result in subsequent calculations of transport processes—a difficulty which can conveniently be deferred to another publication. The nature of the difficulty is easy to state: In order to do a calculation the drift velocity $\vec{v}$ in (1.3) must be determined; any procedure for this will involve calculating various moments of the distribution function and the computation of these moments becomes more cumbersome if Γ depends on wave vector and polarization.

2. Umklapp processes

Since umklapp processes involve the transfer of momentum to the lattice they tend to relax the phonons to that frame—i.e., to an equilibrium distribution in the absence of any perturbation. Accordingly the appropriate relaxation-time approximation is

$$I^U(n(\vec{q}\lambda)) = -[n(\vec{q},\lambda) - n_0(\vec{q},\lambda)](2\Gamma^U_{pp}), \qquad (1.4)$$

where $n_0(\vec{q},\lambda) = (e^{\beta\omega(\vec{q},\lambda)} - 1)^{-1}$ is the standard equilibrium distribution. The details of the way we calculate Γ^U_{pp} are specified elsewhere in this paper (see Appendix A).

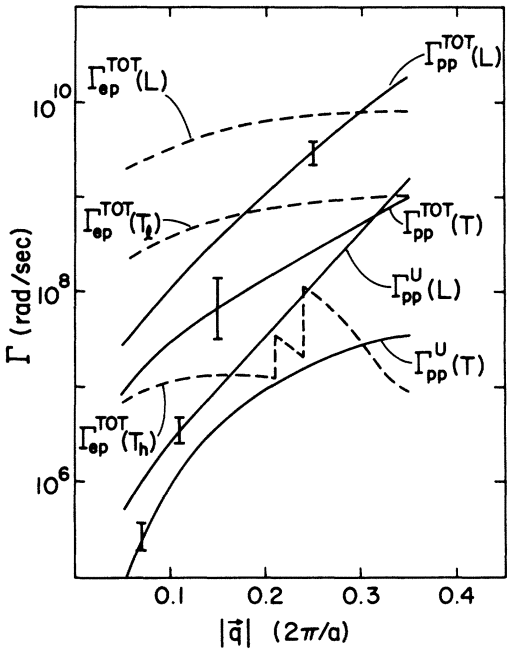

FIG. 2. Semilog plot of the q dependence of Γ^{tot}_{pp}, Γ^{U}_{pp}, and Γ_{ep} at 1 K for potassium. For this temperature Γ_{pp} is roughly independent of direction and the half-widths for the [1 0 0], [1 1 0], and [1 1 1] directions all fall fairly close to a set of "universal" curves, which are those shown above. Maximum scatter about these curves is indicated by the barred lines. For the only symmetry direction, [1 1 0], which has nondegenerate transverse branches, $\Gamma(T_h)$ is sufficiently close to $\Gamma(T_l)$ for the two sets of points to fall within the barred lines on the curves labeled by $\Gamma_{pp}(T)$ for both the total and the umklapp half-widths. As a point of reference we also show the electron-phonon half-widths $\Gamma_{ep}(L)$ and $\Gamma_{ep}(T)$ for the [6 2 1] direction. Γ_{ep}'s are temperature independent. [6 2 1] direction was chosen so as to avoid effects associated with the symmetry directions (see Secs. III and IV for further details on this point). The discontinuities in Γ_{ep} are due to umklapp processes turning on.

Although there have been many theoretical discussions of the separation of decay rates into Γ^N_{pp} and Γ^U_{pp} and several attempts[11,12] to extract these numbers from experiments, it is somewhat surprising that there has been only one serious microscopic calculation.[13] Niklasson has calculated weighted averages of Γ^{tot}_{pp} and Γ^U_{pp} as a function of temperature for argon, and finds that the ratio Γ^{tot}/Γ^U varies from about 2 at 100 K to about 50 at 5 K. The primary concern of his paper is to explore the differences between ordinary sound and collisionless (or zero or high-frequency) sound. The crossover between these two sounds occurs for $\omega \sim \Gamma^{tot}_{pp}$, so that the calculation of Γ^U_{pp} plays a role only in a discussion of some transport properties and the damping of ordinary sound. On the other hand, the bulk of the theoretical interest has been in discovering those systems in which second sound can propagate. The condition for this is $\Gamma^U_{pp} \ll \omega \ll \Gamma^N_{pp}$, and hence the interest in making estimates.

Finally we should point out that bad as our calculation of $\Gamma^N_{pp}(\vec{q},\lambda;T)$ and $\Gamma^U_{pp}(\vec{q},\lambda;T)$ may be, they are the first that have, as far as we know, ever been attempted.

C. Summary of results

In Fig. 2 we have attempted to represent schematically many of the results of our calculation. With some discussion it will be possible to extract additional information from Fig. 2.

1. Phonon-phonon scattering Γ_{pp}

The four solid curves in Fig. 2 give the wave-vector ($\vec{q}$) dependence of phonon-phonon scattering *at one temperature* (1 K). The total and umklapp rates for the longitudinal and transverse phonons are given. These "universal" curves represent an average value of the results calculated along the [100], [110], and [111] directions. The "scatter" around these curves is indicated by the barred line. Two features are clear: (i) Any given rate is relatively independent of the *direction* of $\vec{q}$, and (ii) there is some dependence on the magnitude of $\vec{q}$ associated with the polarization.

What is not on the figure is the strong temperature dependence of the Γ_{pp}. All the rates increase with the temperature with the low-q end being raised most rapidly and with the difference both

TABLE I. q dependence of the normal (N) and umklapp (U) contribution to both the longitudinal (L) and the transverse (T) phonon-phonon half-widths in the [ξ 0 0] direction at 1 and 92 K. Calculations used a 1024-point mesh and $\epsilon = 6.5 \times 10^{11}$ rad/sec (see Appendix A for a discussion of the mesh size and ϵ). "Higher" and "lower" transverse modes (T_h and T_l) are degenerate in this direction.

Normal	$T=1$ K		$T=92$ K		Umklapp	$T=1$ K		$T=92$ K	
ξ ($2\pi/a$)	Γ_L^N (10^9 rad/sec)	Γ_T^N	Γ_L^N (10^9 rad/sec)	Γ_T^N	ξ ($2\pi/a$)	Γ_L^U (10^9 rad/sec)	Γ_T^U	Γ_L^U (10^9 rad/sec)	Γ_T^U
0.1	0.5	0.1	10	7	1	0.02	0.005	0.4	0.3
0.2	2	0.4	30	30	2	0.2	0.06	3	4
0.4	10	2	80	40	4	0.7	0.7	6	20
0.6	30	7	140	50	6	6	5	30	30
0.8	20	10	70	50	8	30	10	120	50
(ξ, 0, 0)	L	$T_h=T_l$	L	$T_h=T_l$	(ξ, 0, 0)	L	$T_h=T_l$	L	$T_h=T_l$

between Γ^{tot} and Γ^U and between different polarizations being greatly reduced.

2. *Electron-phonon scattering* Γ_{ep}

Up to this point we have said little about electron-phonon scattering. It is relatively simple to calculate, especially since it is essentially temperature independent in most metals. The dashed curves in Fig. 2 show the electron-phonon rates along the [621] direction for longitudinal and transverse phonons. It can be seen that the longitudinal rate is initially proportional to the wave vector. What cannot be seen here is the extreme sensitivity of the transverse phonon rates upon the direction of the phonons. Along symmetry directions the transverse phonon rate is zero for all wave vectors below the value where umklapp processes begin. The larger value of the transverse phonon rate is a consequence of the large anisotropy in the phonon spectrum of potassium, a point which is discussed in detail in Sec. III.

3. *Temperature dependence*

At 1 K we can see in Fig. 2 that $\Gamma_{ep} > \Gamma_{pp}$ for phonons of that energy ($q \sim 0.01 \times 2\pi/a$), but it must be remembered that Γ_{ep} is calculated along a certain direction [621]. Along and near symmetry directions $\Gamma_{ep} < \Gamma_{pp}$ for transverse phonons, so one cannot even conclude that phonon drag dominates at 1 K, although we would suppose that, in the absence of any detailed calculation, phonon-drag effects would play an important role in the transport processes at 1 K. For increasing temperatures all the phonon-phonon scattering rates will increase and at various crossover temperatures each Γ_{pp} process will exceed its appropriate Γ_{ep} process. For potassium we estimate all these "crossovers" will have occurred by about 30 K. Hence at such and higher temperatures the Bloch limit is quite a good one.

The plan of the rest of the paper is as follows: The phonon-phonon and electron-phonon scattering rates are discussed in detail in Secs. II and III, respectively. Section IV contains a comparison of the two rates. Finally in Sec. V we make a tentative extension of the work to another alkali metal, rubidium, and even more tentatively to a polyvalent metal, aluminum. Computational details are relegated to the appendices.

II. PHONON-PHONON HALF-WIDTHS

This section comprises a summary of our calculations for the total phonon-phonon half-width Γ_{pp}^{tot} and the umklapp contribution to the half-width Γ_{pp}^U. A quick glance at our results in their barest form, Tables I–III, indicates the complexity in-

TABLE II. Small-q dependence of the total and umklapp phonon-phonon half-widths in the [ξ 0 0] and [ξ ξ ξ] directions at 1 K. Calculations used an 11 664-point mesh with $\epsilon = 1 \times 10^{11}$ rad/sec.

ξ ($2\pi/a$)	Γ_L^{tot} (10^9 rad/sec)	$\Gamma_{T_h=T_l}^{tot}$	Γ_L^U (10^9 rad/sec)	$\Gamma_{T_h=T_l}^U$	ξ ($2\pi/a$)	Γ_L^{tot} (10^9 rad/sec)	$\Gamma_{T_h=T_l}^{tot}$	Γ_L^U (10^9 rad/sec)	$\Gamma_{T_h=T_l}^U$
0.05	0.03	0.004	0.0003	0.000 07	0.05	0.06	0.03	0.001	0.0004
0.1	0.1	0.02	0.004	0.0009	0.1	1	0.1	0.01	0.004
0.2	1	0.1	0.03	0.009	0.2	19	2	1	0.04
(ξ, 0, 0)	L	$T_h=T_l$	L	$T_h=T_l$	(ξ, ξ, ξ)	L	$T_h=T_l$	L	$T_h=T_l$
	total		umklapp			total		umklapp	

TABLE III. Total and umklapp contributions to the phonon-phonon half-widths for several different temperatures and values of q in the $[\xi\ \xi\ 0]$ direction. As was noted in the text, this is the only high-*symmetry* direction which has three *non*degenerate phonon modes. 11 664-point mesh size was used with $\epsilon = 1\times10^{11}$ rad/sec.

ξ	T	Γ_L^{tot}	$\Gamma_{T_h}^{tot}$	$\Gamma_{T_l}^{tot}$	Γ_L^U	$\Gamma_{T_h}^U$	$\Gamma_{T_l}^U$
$(2\pi/a)$	(K)	(10^9 rad/sec)			(10^9 rad/sec)		
0.05	0.4	0.04	0.01	0.02	...	...	...
	1	0.04	0.01	0.02	0.0005	0.0002	0.0004
	9	0.1	0.08	2	...	...	...
	92	4	4	40	...	...	...
0.1	0.4	0.4	0.06	0.07	...	...	...
	1	0.4	0.06	0.07	0.007	0.003	0.004
	9	0.8	0.2	3	0.01	0.004	0.2
	30	6	3	21	0.4	0.3	2
	92	24	15	71	2	2	6
0.2	0.4	4	0.8	0.2	...	...	...
	1	4	0.8	0.2	0.4	0.03	0.02
	9	4	2	5	0.4	0.07	0.5
	30	14	13	38	1	2	6
	92	47	51	130	5	9	22
0.4	9	28	10	13	12	7	2
	30	45	30	87	19	16	23
	92	120	98	300	48	51	87
$(\xi,\xi,0)$	Temp.	L	T_h	T_l	L	T_h	T_l
		total			umklapp		

volved in trying to interpret these numbers and of trying to compare them with the electron-phonon half-widths. The chief source of this complexity lies in the number of variables on which the half-widths depend. In particular, we have to specify the wave number $\vec{q}$ (including both magnitude and direction), the polarization λ, the temperature T, and also whether we are interested in the total half-width Γ_{pp}^{tot} or just the umklapp contribution Γ_{pp}^U. We remind the reader $\Gamma_{pp}^{tot} = \Gamma_{pp}^N + \Gamma_{pp}^U$; i.e., the total is the sum of the normal and umklapp contributions to Γ_{pp}.

Despite these difficulties, it is possible to develop a semiquantitative picture of how the two kinds of half-width compare with each other by concentrating on how each of them separately depends upon the various variables. Fortunately, it will often turn out that one or the other of the half-widths will be independent of a certain variable, and hence this fact will greatly simplify our task. We now begin this process by considering the dependences of the phonon-phonon half-widths.

a. $\vec{q}$ dependence. Γ_{pp} is a very strong function of the magnitude of q, monotonically increasing by orders of magnitude as $|\vec{q}|$ becomes larger, with the strongest q dependence occurring at the lowest temperatures. This strong dependence on the *magnitude* of $\vec{q}$ usually greatly dominates the dependence of Γ_{pp} on the *direction* of $\vec{q}$, which typically varies by at most a factor of 2. Furthermore Γ_{pp} shows the same qualitative dependence on $|\vec{q}|$ independent of both the polarization and whether we are considering Γ_{pp}^{tot} or Γ_{pp}^U. In all cases Γ_{pp} is a monotonically increasing function of $|\vec{q}|$ with the strongest dependence at small $|\vec{q}|$ and low temperature. At 1 K Γ_{pp}^{tot} and Γ_{pp}^U have a rough power dependence of q^3 to q^4 for $0.1 \lesssim q(a/2\pi) \lesssim 0.3$ for both longitudinal and transverse modes. See Fig. 2. Below $0.1\times 2\pi/a$ the dependence is faster than q^4. As we will see in Sec. III this is much stronger than the linear dependence of $\Gamma_{ep}(q)$.

b. Temperature dependence. Γ_{pp} is strongly temperature dependent, changing by two or three orders of magnitude between 1 and 100 K. At sufficiently low temperatures the curve of Γ_{pp}^{tot} plotted as a function of temperature flattens out and Γ_{pp} approaches a finite zero-temperature limiting value at finite q. See, for example, Fig. 3.

c. Polarization dependence. There is a slight tendency for the total half-width for longitudinal phonons $\Gamma_{pp}^{tot}(L)$ to be larger than that for the transverse phonons $\Gamma_{pp}^{tot}(T)$ at low temperature and *vice versa* at high temperature. In general, the half-widths for the different polarizations tend to stay within an order of magnitude of each other. This lack of any strong patterns in the polarization dependence (for example, with $\vec{q}$) contrasts strongly with the case for $\Gamma_{ep}(q)$.

d. Umklapp contribution. The umklapp contribution is very strongly dependent on the wave num-

ber, temperature, and phonon frequency. The width is largest for large q, especially near the zone boundaries. It drops by orders of magnitude for decreasing q, dropping faster for the high-frequency branches of the phonon spectrum. For small q there is a pronounced temperature dependence whereby $\Gamma_{pp}^{U}/\Gamma_{pp}^{tot}$ decreases rapidly at lower temperatures. At sufficiently large q $\Gamma_{pp}^{U}/\Gamma_{pp}^{tot}$ is essentially temperature independent.

e. Symmetry directions. It should be emphasized that we have only calculated Γ_{pp} along symmetry directions. Although we have no reason to suspect any strange behavior in the phonon-phonon half-widths as we move away from symmetry directions, we are unable to make any definitive statement in this regard without explicit calculation. (A hindrance to such a calculation is that the resulting decay rates are a matrix in the polarization vectors.) The electron-phonon half-width $\Gamma_{ep}(\vec{q})$, on the other hand, is strongly dependent on whether the wave vector $\vec{q}$ lies along a symmetry direction or not, especially for the transverse modes. This point is discussed below.

III. ELECTRON-PHONON HALF-WIDTH

The contribution of electron-phonon scattering to the total phonon width for wave number $\vec{q}$ and polarization λ is given by

$$\frac{1}{\tau_{ep}}(\vec{q},\lambda) = 2\Gamma_{ep}(\vec{q},\lambda) = \frac{m^2}{2\pi\rho\hbar^3}\sum_G |V(Q)|^2 \frac{|\vec{Q}\cdot\hat{\epsilon}_{q\lambda}|^2}{|\vec{Q}|}\Theta(2k_F - Q), \tag{3.1}$$

where m is the mass of an electron, ρ the ion mass density, $V(Q)$ the pseudopotential, $\hat{\epsilon}_{q\lambda}$ the polarization vector of the phonon, $\vec{Q}\equiv\vec{q}+\vec{G}$, $\vec{G}$ a reciprocal-lattice vector, and k_F the Fermi wave number. See Appendices B and C for further details, including a derivation of (3.1).

A. Temperature and q dependence

In contrast to Γ_{pp} the electron-phonon half-width Γ_{ep} has a simple temperature and q dependence. In particular, because the relevant comparison temperature for these processes, the Fermi temperature T_F, is large (~25 000 K) the temperature dependence is negligible. The $\vec{q}$ dependence of Γ_{ep} is given by

$$\Gamma_{ep} \propto q|\hat{q}\cdot\hat{\epsilon}_{q\lambda}|^2 \tag{3.2}$$

in the long-wavelength limit ($q \lesssim 0.3\times 2\pi/a$). This result may easily be derived from (3.1) by noticing that $V(Q)\to -\frac{2}{3}\epsilon_F$ as $Q\to 0$, and that the umklapp contribution is zero for sufficiently small q. The second observation is a consequence of the fact that *no* reciprocal-lattice vector $\vec{G}$ satisfies the geometrical constraint $2k_F \geq |\vec{q}+\vec{G}|$ for sufficiently small q in a material like potassium, whose Fermi surface does *not* touch the Brillouin-zone boundaries. Farther out in the Brillouin zone ($q \gtrsim 0.3\times 2\pi/a$), where it is necessary to include both the umklapp processes and the Q dependence of $V(Q)$ in (3.1), Γ_{ep} is relatively insensitive to q as compared to Γ_{pp}. In particular, Fig. 4 shows that Γ_{ep} usually changes by *less* than an order of magnitude in this region.

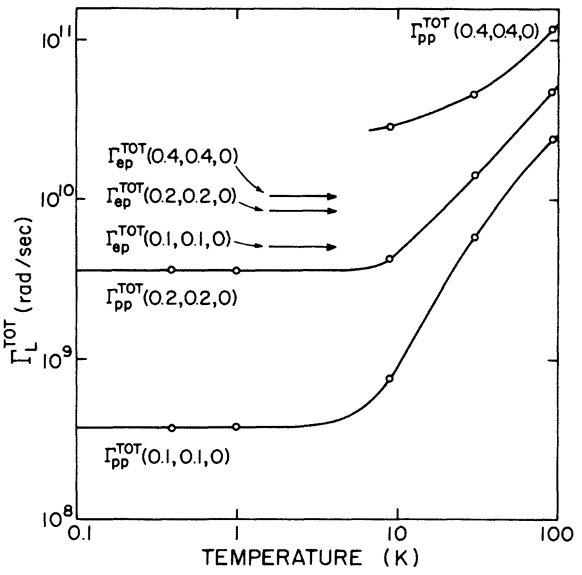

FIG. 3. Plot of $\Gamma_{pp}^{tot}(L)$ as a function of temperature for $\vec{q}=(0.1,\ 0.1,\ 0)(2\pi/a)$, $(0.2,\ 0.2,\ 0)(2\pi/a)$, and $(0.4,\ 0.4,\ 0)(2\pi/a)$. Curves are a rough interpolation between the calculated points marked by the circles. Calculations for these points used an 11 664-point mesh size with $\epsilon = 1\times 10^{11}$ rad/sec. Temperature-independent values of $\Gamma_{ep}^{tot}(L)$ for these three wave vectors are indicated by the arrows in the middle of the figure. [Intersection of these values with the plot of Γ_{pp}^{tot} as a function of temperature for fixed $\vec{q}$ defines the crossover temperature T_{cr} (see Sec. IV) which is plotted in Fig. 9.]

B. Directional dependence—long-wavelength region ($q \lesssim 0.3 \times 2\pi/a$)

We turn now to the strong dependence of Γ_{ep} on the direction of $\vec{q}$ in the low-wavelength limit. We observe that this is the appropriate region of interest; at temperatures $\lesssim$30 K, i.e., in the temperature range at which Γ_{ep} begins to become comparable to Γ_{pp} (see Sec. IV), thermal phonons will typically have wave numbers of less than $0.3\times 2\pi/a$ (cf. Fig. 5).

This directional dependence is determined by the polarization vectors via the $|\hat{q}\cdot\hat{\epsilon}_{q\lambda}|^2$ factor in (3.2). The dependence is particularly pronounced in the case of transverse phonons along symmetry directions where $|\hat{a}\cdot\hat{\epsilon}_{q\lambda}|\to 0$ and hence $\Gamma_{ep}\to 0$.

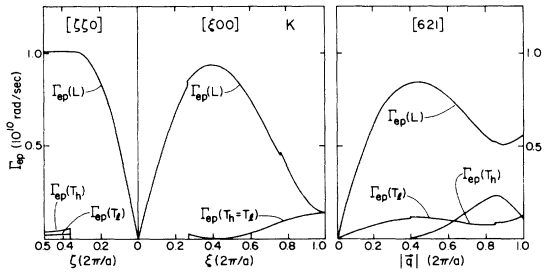

FIG. 4. q-dependence of the electron-phonon half-width Γ_{ep}^{tot} in the [1 0 0], [1 1 0], and [6 2 1] directions for potassium. As was explained in the text these results are nearly temperature independent. Degeneracy of the half-widths Γ_{ep}^{tot} at the point $(1,0,0)(2\pi/a)$ is exact. At this point only $|\vec{Q}| = |\vec{q}+\vec{G}| = 2\pi/a$ wave vectors are involved in the sum over $\vec{G}$ in Eq. (3.1), resulting in the same value of Γ_{ep}^{tot} for the longitudinal and transverse modes. A similar degeneracy occurs at (0.5, 0.5, 0.5) $(2\pi/a)$ (not shown), where only wave vectors $|\vec{Q}| = 0.866 \times 2\pi/a$ are involved.

Off symmetry directions Γ_{ep} are not zero for these phonons, but this factor still causes the half-width to be much smaller than for the longitudinal phonons even when the polarization vector is far from being transverse. For example, $\hat{\epsilon}_{q\lambda}$ has to deviate from a plane perpendicular to $\vec{q}$ by as much as 18° before $|\hat{q}\cdot\hat{\epsilon}_{qT}|^2 = \frac{1}{10}$, i.e., before $\Gamma_{ep}(T)$ is within an order of magnitude of $\Gamma_{ep}(L)$ (note that $|\hat{q}\cdot\hat{\epsilon}_{qL}|$ lies within a few percent of unity for all q directions).

In studying the directional dependence of the transverse phonons via the polarization vectors, it it sufficient for our purposes to look only at the long-wavelength limit, i.e., for $q \lesssim 0.3\times 2\pi/a$. In this region the polarization vectors obtained by a Born–von Kármán analysis fitted to inelastic neutron data are roughly q independent and fit smoothly

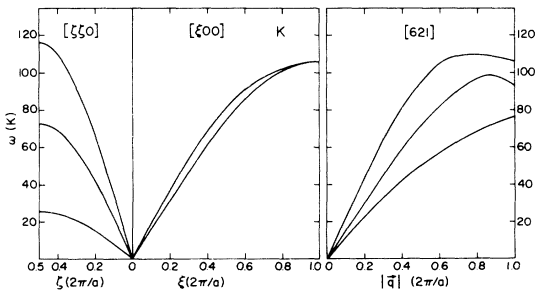

FIG. 5. Dispersion curves for potassium in the [1 0 0], [1 1 0], and [6 2 1] directions. Curves were obtained by using a Born–von Karman analysis fitted to inelastic neutron data. See, for example, Ref. 6(a). Phonon frequencies are plotted in temperature units (i.e., $T=\hbar\omega/k_B$). [1 0 0] direction (like the [1 1 1] direction which is not shown here) has two degenerate transverse modes.

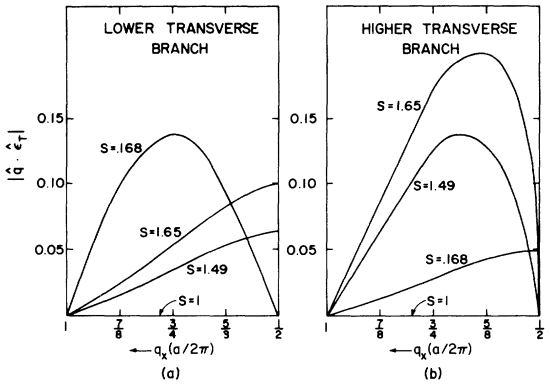

FIG. 6. $|\hat{q}\cdot\hat{\epsilon}_T|$ for the lower and higher transverse modes for different values of the anisotropy index s in the directions defined by q_x, $q_y = 2\pi/a - q_x$, and $q_z = \frac{1}{2}q_y$. These directions correspond to points lying on the line AD of Fig. 7. Curves were calculated in the long-wavelength limit using the elastic constants of tungsten for c_{11} and c_{44}. c_{12} was adjusted to change s. For $s=1$ (which is the case for tungsten) the system is isotropic and for both transverse modes $|\hat{q}\cdot\hat{\epsilon}_T| = 0$ for all $\vec{q}$. See the text for further details.

onto those determined from the elastic constants (i.e., the long-wavelength limit). In this limit they depend crucially upon the ratios of the elastic contants c_{11}, c_{44}, and c_{12}. In particular their behavior is largely determined by the anisotropy index s which is defined by[14]

$$s \equiv (c_{11}-c_{12})/2c_{44}, \tag{3.3}$$

and whose deviation from unity is a measure of the system's elastic anisotropy.

C. "Anisotropic" tungsten model

To illustrate the dependence of the polarization vectors on s we consider a model of tungsten (normally a bcc metal with $s=1$) in which we kept c_{11} and c_{44} fixed[15] and hence left unchanged the longitudinal and transverse velocities in the [001] direction and varied s above and below unity. (The only constraint on s, imposed by the stability condition $c_{11}+2c_{12}>0$, is that $s < 3c_{11}/4c_{44} = 2.4$ for tungsten.) Figure 6 shows the effects of this variation on the higher and lower transverse polarizations.

In these figures and several others (for potassium) we have used the convention that the direction of $\vec{q}$ is determined by the coordinates of the point on the faces of the Brillouin zone which a ray in the direction of $\hat{q}$ would intersect. Since we restrict ourselves to the $\frac{1}{48}$th irreducible part of the Brillouin zone, this means that all such points will lie in the plane ANP of Fig. 7. For example, the [110] direction is specified by the point $(\frac{1}{2}, \frac{1}{2}, 0)$, the [621] direction by the point $(\frac{3}{4}, \frac{1}{4}, \frac{1}{8})$, etc.

Figure 6 is a plot of $|\hat{q}\cdot\hat{\epsilon}_{T_h}|$ and $|\hat{q}\cdot\hat{\epsilon}_{T_l}|$, in

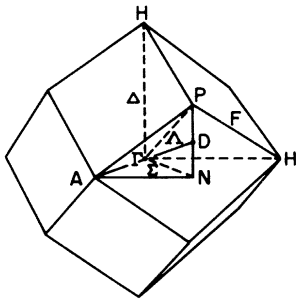

FIG. 7. Brillouin zone (in reciprocal space) for a body-centered cubic lattice (which is the case for potassium). Prism-shaped volume defined by the points A, N, P, and Γ is the $\frac{1}{48}$th irreducible part of the zone. Several points and lines of symmetry are indicated as well as a few additional points which are referred to in the text. We choose our coordinate axes so that $A = (1,0,0)$, $N = (\frac{1}{2},\frac{1}{2},0)$ and $P = (\frac{1}{2},\frac{1}{2},\frac{1}{2})$ in units of $2\pi/a$.

the long-wavelength limit, for directions corresponding to points lying on the line AD of Fig. 7, i.e., roughly through the middle of the $\frac{1}{48}$th irreducible section of the Brillouin zone. We have not bothered to give a third plot for the longitudinal polarization vectors since $|\hat{q}\cdot\hat{\epsilon}_L| \approx 1$ for any value of s.

An examination of Fig. 6 shows that when s deviates from unity, large changes occur in $|\hat{q}\cdot\hat{\epsilon}_T|$ along nonsymmetry directions. Furthermore we would point out but can not explain a kind of "conjugate" behavior between the behavior of $\hat{\epsilon}_{T_h}$ and $\hat{\epsilon}_{T_l}$ as s varies from below unity to above it. By this we mean that $|\hat{q}\cdot\hat{\epsilon}_{T_h}|$ for $s>1$ looks similar to the curves of $|\hat{q}\cdot\hat{\epsilon}_{T_l}|$ for $s<1$ and *vice versa*. For $s=1$ $|\hat{q}\cdot\hat{\epsilon}_{T_h}| = |\hat{q}\cdot\hat{\epsilon}_{T_l}| = 0$ and the two curves join together.

D. Potassium

Potassium corresponds to a value of $s=0.131$. On the basis of Fig. 6 we are led to believe that the deviations of $|\hat{q}\cdot\hat{\epsilon}_{T_l}|$ from zero will be much larger than the deviations of $|\hat{q}\cdot\hat{\epsilon}_{T_h}|$. This conclusion is borne out by detailed calculations using the correct elastic constants for potassium.[16] The results are shown in Fig. 8, where we have plotted "equal-value" curves of $|\hat{q}\cdot\hat{\epsilon}_T|$ as a function of direction within the $\frac{1}{48}$th irreducible part of the Brillouin zone. The convention for determining the direction is the same as is used for Fig. 6.

Figure 8 clearly shows that while the higher transverse mode (T_h) is almost always close to being purely transverse in all directions, the *lower* transverse mode (T_l) deviates quite a bit with $|\hat{q}\cdot\hat{\epsilon}_{T_l}| \sim 0.3$ over most directions which are not lines of symmetry. Consequently Γ_{ep} for the lower transverse mode retains a surprising amount of strength even in the $q\to 0$ limit [see Eq. (3.2)]. As a point of reference note that a Debye model would predict $\Gamma_{ep}=0$ for all transverse phonons in the absence of umklapp processes since it requires $|\hat{q}\cdot\hat{\epsilon}_T| = 0$. In sharp contrast to the off-symmetry directions, the electron-phonon half-width for transverse phonons, $\Gamma_{ep}(T)$, is zero along symmetry directions for $q\to 0$ since symmetry then requires $|\hat{q}\cdot\hat{\epsilon}_T| = 0$. In this latter case $\Gamma_{ep}(T)$ therefore can only turn on at finite q (e.g., at $q = 0.27\times 2\pi/a$ in the [100] direction) when umklapp processes become possible.

IV. Γ_{ep}-Γ_{pp} COMPARISON

Figures 9 and 10 summarize the results of our comparison between Γ_{ep} and Γ_{pp}. The solid line in Fig. 9 is a plot of the crossover temperature T_{cr} as a function of wave vector q. It is defined by

$$\Gamma_{pp}^{tot}(q,\lambda;T_{cr}) = \Gamma_{ep}^{tot}(q,\lambda). \tag{4.1}$$

As we have discussed in Sec. III, the electron-phonon half-width Γ_{ep} is independent of temperature.

The solutions to (4.1) were obtained graphically, with necessary interpolations being made between the points (q, T) for which we have calculated Γ_{pp}.

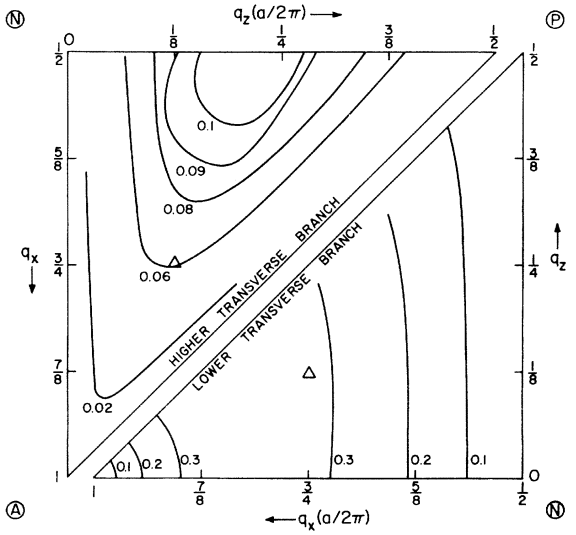

FIG. 8. "Equal-value" curves of $|\hat{q}\cdot\hat{\epsilon}_T|$ in the long-wavelength limit for potassium as a function of direction (within $\frac{1}{48}$ irreducible part of the Brillouin zone). The notation used for direction is explained in the text. Points labeled by the circled letters, A, N, and P refer to the directions ΓA, ΓN, and ΓP indicated in Fig. 7. We remind the reader that $q_y = 2\pi/a - q_x$ in these plots. Triangular-shaped region in the upper left-hand corner gives values for the higher transverse branch and the lower right-hand region gives values for the lower transverse branch. In order to save space we have labeled the various axes in such a way that the two triangular regions are mirror images of each other. Intersection of the [6 2 1] direction with the ANP plane is labeled by a triangle (Δ).

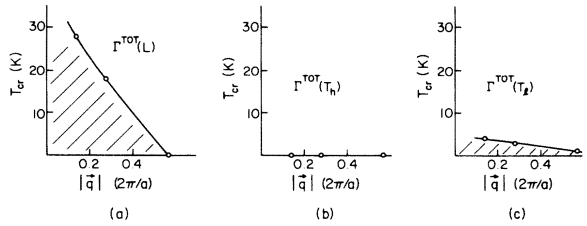

FIG. 9. Rough comparison between Γ_{pp}^{tot} and Γ_{ep}^{tot} as a function of temperature and wave number. Solid curve is a crude estimate of the crossover temperature T_{cr}, for which $\Gamma_{ep}^{tot} = \Gamma_{pp}^{tot}$ at fixed q. At temperatures less than T_{cr} (the shaded area in the figures) $\Gamma_{ep}^{tot} > \Gamma_{pp}^{tot}$. At temperatures greater than T_{cr} the reverse is true, $\Gamma_{ep}^{tot} < \Gamma_{pp}^{tot}$. In each figure, the curve passing through the three calculated crossover points (indicated as circles) is included as a guide to the eye. Note that in (b) the circles all lie on the abscissa, indicating, that within the accuracy of the calculations, $\Gamma_{pp} > \Gamma_{ep}$. See, for example, the calculated rates for the point (0.4, 0.4, 0) $(2\pi/a)$ in Fig. 3.

A typical example is shown in Fig. 3. At temperatures below the solid line $T_{cr}(q)$, i.e., in the shaded area of the figures, $\Gamma_{ep}^{tot}(q) > \Gamma_{pp}^{tot}(q, T)$. For temperatures above the solid line $\Gamma_{ep}^{tot}(q) < \Gamma_{pp}^{tot}(q, T)$. In those cases where, within the limited accuracy and range (in $\vec{q}$ and T) of the calculations, the phonon-phonon rate always exceeds the electron-phonon one as in Fig. 9(b), $T_{cr}(q)$ is then set equal to zero. Figure 10, which compares the umklapp contribution to the phonon-phonon half-width Γ_{pp}^{U} with Γ_{ep}^{tot}, uses the same conventions as Fig. 9. The reader should be warned that a detailed comparison is more complex than is suggested by these figures. We shall return to this point shortly. Furthermore, the accuracy of the numbers for Γ_{pp} at low temperatures is not known very well (see Appendix A) and better calculations may eventually cause the curves to shift. Since our experience with the effects of mesh size leads us to believe that in most cases we overestimate Γ_{pp}, if there is a shift it should in most cases probably be upward for $T_{cr}(q)$.

For the longitudinal phonons the graphs in these figures are based on calculations of Γ_{pp} and Γ_{ep} in the [110] direction. This direction is singled out because, as noted earlier, it is the only symmetry direction that has three *nondegenerate* phonon modes. (We remind the reader that we have not calculated Γ_{pp} in nonsymmetry directions.) For the transverse phonons the graphs are again based on calculations of Γ_{pp} in the [110] direction, but this time Γ_{ep} is taken from calculations in the [621] direction [where we have solved (4.1) for the same *magnitude* of q]. The reason for choosing the [621] direction is that it lies roughly in the middle of the $\frac{1}{48}$th irreducible part of the Brillouin zone and may be considered to give a "typical" value for $\Gamma_{ep}(T)$. There is no point in using the [110] direction for Γ_{ep} for transverse phonons since it is zero in the long-wavelength limit. Since Γ_{ep} is essentially independent of direction for longitudinal phonons in the long-wavelength limit (this is a consequence of the empirical fact that $|\hat{q} \cdot \hat{\epsilon}_L| \sim 1$ for all directions) no such problem arises in the longitudinal case.

From this discussion it is clear that Figs. 9 and 10 represent only a rough estimate of how Γ_{pp} and Γ_{ep} compare at different values of q and temperature for "typical phonons." Direction plays an exceedingly important role for the transverse modes. Along certain symmetry directions $\Gamma_{pp}(T)$ is always greater than $\Gamma_{ep}(T)$ even at zero temperature, whereas away from symmetry directions the situation may reverse with $\Gamma_{ep}(T) \gg \Gamma_{pp}(T)$.

The picture that seems to be emerging from these calculations is as follows. At high temperature, say above 30 K, Γ_{pp} dominates Γ_{ep} and the phonon system will be in equilibrium with itself. It is in this region where it is permissible to use Bloch's "Annahme," which states that the phonon distribution function can be taken to be that of the equilibrium phonon distribution.[17]

In the region below 30 K, say down to 1 K, the situation becomes complex. The coupling to the electron system via Γ_{ep} will be of the same order of magnitude as the coupling among the phonons via Γ_{pp}. If, for example, momentum is fed into the electron system via an electric field, this *may* lead to a steady-state phonon distribution function which has a net momentum associated with it. Any attempt to figure out whether this will or will not happen is complicated by the fact that some modes may be in thermal equilibrium while others are strongly "dragged" by the electron system. For example, at 10 K Fig. 9 predicts that $\Gamma_{ep}^{tot} > \Gamma_{pp}^{tot}$

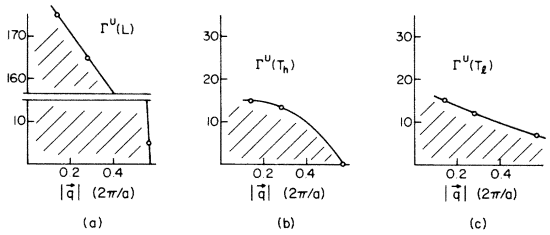

FIG. 10. Rough comparison between the umklapp contribution to the phonon-phonon half-width Γ_{pp}^{U} and Γ_{ep}^{tot}. Solid curve is a crude estimate of the crossover temperature T_{cr} at which $\Gamma_{ep}^{tot} = \Gamma_{pp}^{U}$ at fixed $\vec{q}$. At lower temperatures (the shaded area in the figures) $\Gamma_{ep}^{tot} > T_{pp}^{U}$ and at higher temperatures $\Gamma_{ep}^{tot} < \Gamma_{pp}^{U}$. Curve sketched through the three points marked by circles in each figure is included to guide the eye. Note the break in the vertical scale of (a).

for longitudinal (thermal) phonons whereas $\Gamma_{ep}^{tot} < \Gamma_{pp}^{tot}$ for the transverse (thermal) phonons. The situation is even further complicated in the particular case of "drag" effects in the electrical conductivity, where it is important to consider also the strength of the umklapp contribution to the phonon-phonon half-width Γ_{pp}^{U}, which at 10 K is less than Γ_{ep} for all three modes. This raises the possibility that, although the phonons for some modes scatter among themselves more rapidly than against the electrons, nevertheless they might not be able to get rid of the extra momentum passed on to them by the electron system because there are insufficient umklapp collisions to dissipate the momentum. Finally it is once again necessary to remember that Γ_{ep} is zero along certain symmetry directions so that the phonons are always in equilibrium among themselves near these directions. These phonons *may* ultimately act as sinks for the momentum by some sort of "convective" process (in momentum space) whereby the phonons in other directions with small umklapp rates relative to electron-phonon scattering are eventually able to dissipate, by normal scattering into these symmetry directions, the momentum acquired from the electron system. At temperatures below 1 K this kind of process may be the dominant mechanism for removing momentum from the system.

V. COMPARISON WITH RUBIDIUM AND ALUMINUM

We turn finally to the question of whether the analysis for potassium is unique, or whether it may also apply to other simple metals. Here we briefly examine the crystal dynamics and electron-phonon scattering rates of rubidium and aluminum. Our chief reason for selecting these two particular examples is the existence of calculations and some experimental measurements of the phonon spectrums, phonon-phonon half-widths (albeit at higher temperatures and larger wave number than we would like), and electron-phonon half-widths of these two materials. We find that, for one of these metals, rubidium, our analysis is almost identical to that for potassium, whereas for aluminum it may turn out that phonon-drag effects are negligible.

A. Rubidium

Like potassium, rubidium has a bcc crystal structure and is monovalent with a Fermi surface which, although slightly more distorted than that of potassium, is approximately spherical and does not cut any zone boundaries. The chief difference between potassium and rubidium appears to result from the different ionic masses (39.1 amu for potassium and 85.47 amu for Rb). The similarities between the two materials shows up clearly in a comparison of the phonon spectra, which are essentially identical[18] except for a scale change due to the different ionic masses ($\omega_{Debye} \sim M^{-1/2}$). The Debye temperature of potassium is 91 K and is 56 K for rubidium.

The phonon-phonon half-widths of rubidium at high temperatures (100, 200, and 300 K) were calculated by Copley,[19] and are readily compared with the high-temperature (92, 215, and 299 K) phonon-phonon half-widths for potassium calculated by Buyers and Cowley.[20] Although there is a great amount of variation from wave vector to wave vector when comparing the two sets of data, the overall trend appears to be that Γ_{pp} for rubidium typically has a value about 60% of that for potassium at the same $\vec{q}$, polarization branch, and similar temperatures (e.g., we compared the 92-K results for potassium with the 100-K results for rubidium, etc). The deviation between the Γ_{pp} for the two alkali metals is least at small q ($\sim 0.2 \times 2\pi/a$).

Using various approximations (e.g., using an isotropic Debye-like phonon spectrum) Kashcheev and Krivoglaz[2] show that $\Gamma \sim |\Phi|^2 C^{-5} T$ in the high-temperature limit ($T \gg \Theta$). Φ is defined in Appendix A, Eq. (A1),[21] and has an explicit ionic mass dependence of $M^{-3/2}$. C is the sound velocity and has an ionic mass dependence $C \sim M^{-1/2}$. Consequently we would expect $\Gamma \sim M^{-1/2}$, all other things being equal. This result agrees well with the overall trend observed in the comparison between rubidium and potassium for the calculation of Γ_{pp}.

The electron-phonon half-widths for rubidium are shown in Fig. 11. They were calculated in the same manner as for potassium [Eq. (3.1)]. The chief difference is a scale reduction (about 46%) which follows from the fact that $\Gamma_{ep} \sim M^{-1}$.

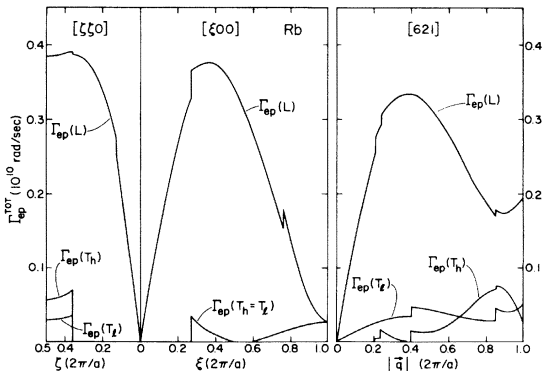

FIG. 11. q dependence of the electron-phonon half-widths for *rubidium* in the [1 1 0], [1 0 0], and [6 2 1] directions. Sharp discontinuities in the curves represent umklapp processes turning on. Because these onsets are determined by purely geometrical considerations, they occur at the same place (in units of $2\pi/a$ in $\vec{q}$ space) as they do for potassium, which also has a bcc crystal structure.

Also the sharp discontinuities, which represent various umklapp processes turning on, are more pronounced in Rb as a consequence of its pseudopotential being a little bigger at $2k_F$ than that of potassium. The anisotropy index for rubidium[22] ($s = 0.124$) is comparable to that of potassium ($s = 0.131$), and consequently the polarization vectors in the long-wavelength limit are also very similar to those of potassium.

The net conclusion from all this analysis is that we expect rubidium to behave essentially the same as potassium with respect to its electron-phonon and phonon-phonon half-widths. Since we do not have any calculations of the low-temperature, small-$\vec{q}$ limit of the phonon-phonon half-widths it is difficult to say whether the crossover temperatures T_{cr} will shift very much from those calculated for potassium. One might guess that the crossover takes place at roughly the same fraction of the Debye temperatures (i.e., would be at about 60% of those for potassium), but the true state of affairs depends on the relative reduction of the phonon-phonon to the electron-phonon rates. We suppose that, with the materials being so similar, the crossover temperatures do not change by more than a factor of 2.

B. Aluminum

Aluminum provides a sharp contrast to both rubidium and potassium. It has a different crystal structure (fcc) with correspondingly different phonon spectrum, but more importantly it is a trivalent metal with a Fermi surface that cuts two zone boundaries. This last point is of great importance, for it means that even for $q \to 0$, umklapp electron-phonon processes provide a low-temperature mechanism for relaxing momentum even in the absence of phonon-phonon umklapp processes. How important this mechanism is depends upon how strong these rates are. Unfortunately there are no good calculations of these rates. All existing calculations[23] that we know of use only one (orthogonalized) plane wave in calculating the appropriate matrix elements and hence are probably inadequate. We will do a similar calculation (as for potassium) in order to provide at least a rough estimate of the possible magnitude of the rate and briefly compare our results with previous calculations.

Högberg and Sandström[9] have calculated the phonon-phonon half-widths of aluminum at 80 and 300 K and compared their results with the experimental data of Stedman and Nilsson.[24] More recent calculations have been performed by Koehler, Gillis, and Wallace[10] which disagree with those of Högberg and Sandström. Unfortunately, Koehler *et al.* only calculate the relative difference in Γ_{pp} between 80 and 300 K without providing absolute values at either temperature. At 80 K the calculations of Högberg and Sandström typically range from being roughly one-half of the experimental width to being comparable with it. The experimental half-widths, which are an upper limit to the two kinds of half-widths, range roughly from 1.4×10^{11} to 1.3×10^{12} rad/sec for $q \gtrsim 0.2\times 2\pi/a$.

Using (3.1) we have calculated Γ_{ep} along the [100] direction for longitudinal phonons. The results are shown in Fig. 12, where we have shown both

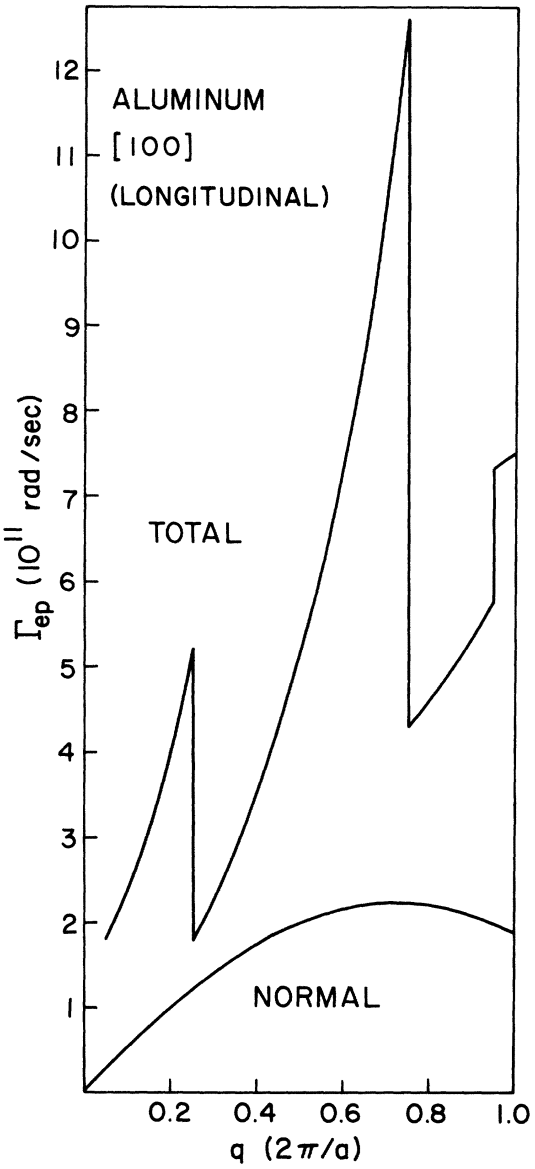

FIG. 12. q dependence of the electron-phonon half-widths in aluminum for longitudinal phonons in the [1 0 0] direction. Sharp discontinuities again represent umklapp processes turning on, but occur in different places than they do for potassium or rubidium since aluminum has an fcc crystal structure. Calculation is very crude and should not be taken too seriously.

the normal contribution and the total electron-phonon half-widths. Our values for normal contribution Γ_{ep}^{N} are roughly comparable to the total half-widths calculated by Björkman *et al.*,[23] who state that in their calculation the main contribution comes from normal processes. Our calculations, however, give a large contribution from umklapp processes. This difference between our results and those of Björkman *et al.* probably means that their effective pseudopotential was much weaker than ours at $q \approx 2k_F$. As Fig. 12 shows, Γ_{ep}^{N} ranges from 1×10^{11} to 2×10^{11} rad/sec, whereas including umklapp processes $\Gamma_{ep}^{\mathrm{tot}}$ can get as high as 10^{12} rad/sec for $q \gtrsim 0.2\times 2\pi/a$. These results suggest that $\Gamma_{ep}^{\mathrm{tot}}$ is roughly between a fifth and a half of Γ_{exp}, and hence $\Gamma_{ep}^{\mathrm{tot}}$ is starting to become comparable with $\Gamma_{pp}^{\mathrm{tot}}$ for longitudinal phonons at 80 K. We remind the reader that $\Theta_{\mathrm{Debye}} \approx 430$ K for aluminum.

As we mentioned earlier, the relative size of the umklapp contribution of Γ_{ep} is important for determining the possibility of phonon drag in aluminum. Our crude calculation, in contrast to that of Björkman *et al.*, suggests that this contribution is rather large. To determine this point it is necessary to do a better job in calculating Γ_{ep} that we have done. Specifically, both a more accurate matrix element and the distorted-Fermi-surface shape must be taken into account. We conjecture that the resulting umklapp rates will be sufficiently large to bring quickly the phonons into equilibrium with the lattice so that the phonon-drag effects will be negligible, but we will not be surprised if this very preliminary analysis has missed some important point.

ACKNOWLEDGMENTS

Two of the authors (R. C. A. and J. W. W.) are grateful for the hospitality of the Institute of Theoretical Physics, Chalmers University of Technology, Göteborg, Sweden, where this project was initiated. Computer funds from the Department of Physics, Umeå University, Umeå, Sweden, were essential to the phonon-phonon calculations, for which the computer codes of Ingvar Ebbsjö, A. B. Atomenergi, Studevik, Nyköping, Sweden, were used. We wish to thank the following for useful discussions and correspondence: W. J. L. Buyers, E. Roger Cowley, Roger A. Cowley, Ingvar Ebbsjö, J. A. Krumhansl, Bengt Lundqvist, Humphrey Maris, Göran Niklasson, and Alf Sjölander.

APPENDIX A: CALCULATION OF PHONON-PHONON HALF-WIDTHS

The phonon-phonon half-widths were calculated using the standard formula[21]

$$\Gamma(k\lambda\omega_{k\lambda}) = \frac{\pi\hbar}{16N\omega(k\lambda)} \sum_{k_1k_2\lambda_1\lambda_2} \Delta(-\vec{k}+\vec{k}_1+\vec{k}_2) \times \frac{|\Phi(-k\lambda; k_1\lambda_1; k_2\lambda_2)|^2}{\omega(k_1\lambda_1)\,\omega(k_2\lambda_2)} \left[-(n_1+n_2+1)\,\delta(\omega+\omega_1+\omega_2)\right.$$

$$\left. +(n_1+n_2+1)\,\delta(\omega-\omega_1-\omega_2) - (n_1-n_2)\,\delta(\omega-\omega_1+\omega_2) + (n_1-n_2)\,\delta(\omega+\omega_1+\omega_2)\right]. \quad \text{(A1)}$$

$\Phi(-\vec{k}\lambda; \vec{k}_1\lambda_1; \vec{k}_2\lambda_2)$ was calculated using a centrosymmetrical potential.[25] The effective potential $V(|\vec{r}|)$ and its spatial derivative were used directly, and the lattice sums were done in coordinate space using three shells of nearest neighbors. For a comparison between the advantages of using real-space versus reciprocal-space lattice sums see Koehler *et al.*[10]

The potential used is that of Buyers and Cowley.[20] To put it into the proper form for our calculations the following procedure was used. Figure 2 on p. 758 of the Buyers and Cowley paper was photographed and enlarged to determine $G(q)$, which is related to the interionic potential $V(q)$ by the formula

$$G(q) = (q^2/z^2e^2)\,V(q). \quad \text{(A2)}$$

To obtain the real-space potential $V(r)$ this expression was Fourier transformed as

$$V(r) = \frac{z^2e^2}{r^2}\left[1 - \frac{2}{\pi}\int_0^\infty \frac{\sin\theta}{\theta}\left(1 - \frac{G(\theta/r)}{4\pi}\right) d\theta\right]. \quad \text{(A3)}$$

The results for $V(r)$ and its spatial derivatives are shown in Fig. 13 and Table IV.

Once the potential is calculated the numerical determination of the phonon-phonon half-width Γ_{pp} for a phonon l by three-phonon processes is determined in the usual fashion by an integration procedure[26] over the other two phonons l' and l''. We use here the abbreviated notation that l stands for the polarization of the phonon mode (longitudinal, L; higher transverse, T_h; lower transverse mode, T_l), the wave vector $\vec{q}$, and frequency $\omega(q\lambda)$. In particular, we construct a uniform cubic mesh in the irreducible $\frac{1}{48}$th volume of the first Brillouin zone. The value of $\vec{q}'$ (the wave vector of phonon l') is determined by methodically selecting points from this mesh. Symmetry operations enable us to cover the entire zone. The wave vector for phonon l'' is constructed by conservation of crystal momentum. If $\vec{q}''$ lies in the first Brillouin zone, the contribution of this process is labeled normal. If it is necessary to reduce $\vec{q}''$ to the first zone by

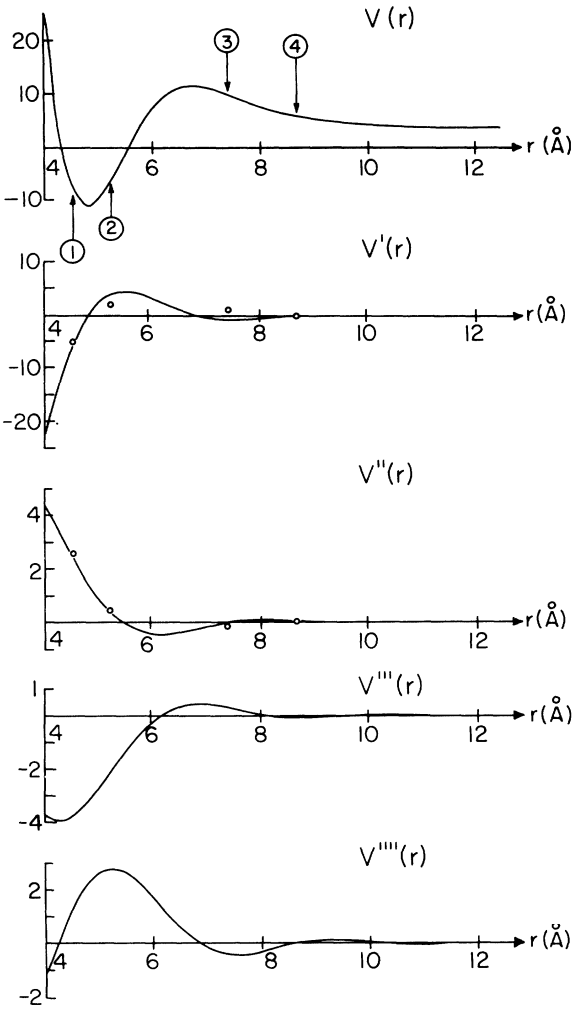

FIG. 13. Plots of the effective potential $V(r)$ and its first four derivatives for potassium, for which points the numerical values are reported in Table IV. Lattice constant $a = 5.2259$ Å. Arrows indicate nearest-neighbor positions. Circles represent the values reported by Cowley, Woods, and Dolling, Ref. 5(a), p. 490, Table II. $V(r)$ is in units of rydbergs, $V'(r)$ in 10^{-6} erg cm^{-1}, $V''(r)$ in 10^{+3} erg cm^{-2}, $V'''(r)$ in 10^{+11} erg cm^{-3}, and $V''''(r)$ in 10^{+19} erg cm^{-4}.

a reciprocal-lattice vector it is labeled umklapp. Once the wave vectors of l' and l'' are established the appropriate eigenvectors, phonon frequencies, thermal factors, matrix elements, etc., are calculated to give the contribution to $\Gamma_{pp}(l)$.

For our purposes it is important to realize that conservation of phonon energy is achieved via a weighting factor

$$\delta(\Delta\omega) = \frac{1}{\pi}\frac{\epsilon}{(\Delta\omega)^2+\epsilon^2} \quad , \tag{A4}$$

where ϵ is a parameter which gives a measure of the sharpness of the conservation law and $\Delta\omega = \omega + \omega' - \omega''$, for example. In the limit $\epsilon \to 0$, this weighting factor is equivalent to the δ function.

Two points should be made regarding this weighting function. First, each of the three phonons involved has a width. Consequently one expects contributions from phonon processes when $\Delta\omega$ is less than or comparable to the largest width of the three phonons involved, with a stronger weighting being given to those processes where $\Delta\omega$ is closer to zero. This sets a scale for ϵ. Second, even if the phonons had no width, for practical considerations some sort of approximation would be required for the δ function representing conservation of phonon energy in order to do the integrations numerically.[27]

The size of ϵ plays an important role with regard to the second point. As ϵ is reduced, fewer points in the integration mesh will give a significant contribution to Γ_{pp}, and the sampling over the region where the integrand is large will become worse, leading to a greater error in the numerical integration. To offset this problem it is necessary to use a finer mesh when ϵ is reduced. This point brings us to crucial problem of mesh size which, as we will subsequently show, becomes the limiting factor which determines the range of temperature and wave vector over which our calculations are feasible.

There are two relevant aspects to this problem. he first is numerical in nature. We need a sufficiently fine mesh for an accurate numerical integration. This size depends not only on the value of ϵ but also occasionally on the size of $\vec{q}$ as well. For example, at low temperatures and for small $\vec{q}$ the largest contribution to the integrand occurs for $\vec{q}'$ and $\vec{q}'' \cong 0$. This requires a fine mesh in order to get an adequate sampling of the $\vec{q}' \sim 0$ region. The second aspect, which is related to the first (the numerical aspect), concerns the physics of the calculation via the importance of choosing a reasonable value of ϵ. As we have noted earlier, ϵ should be of the order of magnitude of the full width of a typical phonon involved in the three-pho-

TABLE IV. First four derivatives of the effective potential $V(r)$ for potassium evaluated at the first three nearest-neighbor distances. nth derivative is in units of erg/cm^n. Lattice constant used in the calculation of the phonon-phonon half-widths was $a = 5.2259$ Å. Mass of the potassium ion was taken to be 6.4922×10^{-23} g.

	1st neighbor	2nd neighbor	3rd neighbor
$V'(r)$	-5.41×10^{-6}	3.83×10^{-6}	-9.28×10^{-7}
$V''(r)$	2.44×10^{3}	3.92×10^{2}	-2.39×10
$V'''(r)$	-3.67×10^{11}	-2.04×10^{11}	2.75×10^{10}
$V''''(r)$	1.41×10^{19}	2.77×10^{19}	-4.30×10^{18}

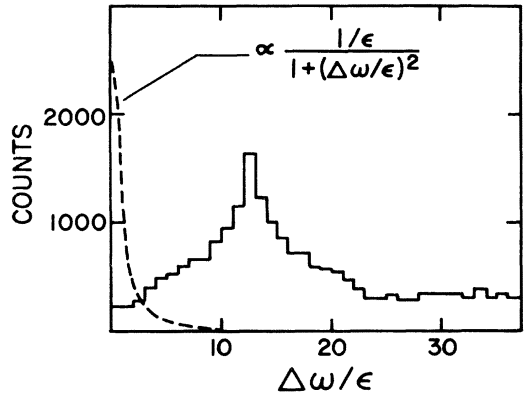

FIG. 14. Number of scattering processes with a given energy difference plotted as a function of how much they deviate from satisfying energy conservation ($\Delta\omega$). Plot was derived from a calculation of the phonon-phonon half-width for $\vec{q}=(0.05,\ 0,\ 0)\ (2\pi/a)$ for the longitudinal branch using a value of $\epsilon = 1\times10^{11}$ rad/sec and a mesh size of 11 664 points in the Brillouin zone. Dashed line in the figure is proportional to $\delta(\Delta\omega)$ [Eq. (A4)] and is provided as a point of reference.

non processes. In the low-temperature limit the widths drop sharply, which requires a very small value for ϵ and hence a fine mesh. With regard to this last point we are in the unfortunate position of needing the low-temperature limit (of the order of 1 K in comparison to a Debye temperature of the order of 100 K) of the phonon-phonon half-width Γ_{pp} since it turns out that it is in this limit that the electron-phonon half-width Γ_{ep} becomes comparable to Γ_{pp}.

In our actual numerical calculations two different mesh sizes and values of ϵ were employed. The larger mesh contained 1024 points in the first Brillouin zone and was used with a value of $\epsilon = 6.5\times10^{11}$ rad/sec (equivalent to 5 K in temperature units). The finer mesh contained 11 664 points and was used with a value of $\epsilon = 1\times10^{11}$ rad/sec (1 K). In each case the value of ϵ was chosen to be as small as possible without damaging the accuracy of the numerical integration.[28]

At high temperatures ($\gtrsim 90$ K) and large wave vector ($\gtrsim 0.2\times2\pi/a$) these mesh sizes and values of ϵ are quite reasonable. Furthermore, for $\vec{q} = (0.2,\ 0.2,\ 0)(2\pi/a)$ and $(0.4,\ 0.4,\ 0)(2\pi/a)$ at 92 K our values of $\Gamma_{pp}^{\rm tot}(T_h)$ using 11 664 points in the Brillouin zone ($\epsilon = 1\times10^{11}$ rad/sec) are essentially identical to those of the calculation of Buyers and Cowley[29] using mesh sizes of 1000 and 2000 points ($\epsilon = 6.5\times10^{11}$ rad/sec), suggesting that the calculations are roughly independent of mesh size and ϵ in this region.

At the lowest temperatures (~ 1 K) and the smallest wave vectors ($\sim 0.5\times2\pi/a$) for which we have calculated, however, neither of these meshes are sufficiently small to give completely reliable results. The finer of our two meshes, for example, corresponds to a spacing between points of the order of $0.04\times2\pi/a$. The values chosen for ϵ are roughly equal to 5 and 1 K in temperature units, and are much larger than typical phonon-phonon half-widths for $T \lesssim 30$ K (cf. the half-widths in Table III with the above values of ϵ).

A good example of the problems that using such a large value of ϵ can lead to is shown in Fig. 14, in which the number of scattering processes are put into bins according to how much they deviate from satisfying energy conservation ($\Delta\omega$). If the number of scattering processes $N(\Delta\omega)$ in the bin $\Delta\omega$ is approximately constant over the range of the weighting factor of (A4), i.e., of the order of 5ϵ, then the weighting factor will correctly give a much stronger weighting to processes which more closely satisfy energy conservation. If, on the other hand, $N(\Delta\omega)$ grows rapidly with $\Delta\omega$ as is shown in Fig. 14, then too much weight will be given to processes which do *not* satisfy energy conservation very well.

Empirically we find that the effect of using too large a value for ϵ (and too coarse a mesh) leads to an *overestimate* of Γ_{pp}. This effect is clearly demonstrated in Table V where we show how Γ_{pp} and Γ_{pp}^{U} vary with mesh size at 1 K. For example, $\Gamma_{Th}^{\rm tot}$ for $\xi = 0.05\times2\pi/a$ in the $[\xi\xi0]$ direction drops one order of magnitude as the mesh size (and ϵ) is changed from 1024 points (6.5×10^{11} rad/sec) to 54 000 points (5×10^{10} rad/sec).[30]

At low temperatures and small q the mesh-size and ϵ problems are not solved easily. For example, by using a uniform mesh even small changes in the mesh spacing lead to a dramatic increase in the number of points in the Brillouin zone. Also, in changing ϵ from 6.5×10^{11} to 5×10^{10} rad/sec we note that we were forced to go from 1024 to 54 000 points in the Brillouin zone in order to get a reasonably accurate numerical integration. To get around these problems it is probably necessary to use a different integration scheme, such as a Monte Carlo program or a logarithmic mesh which, in contrast to a uniform-mesh integration scheme, does not waste a lot of computer time in regions where the integrand is negligible.

APPENDIX B: DERIVATION OF EXPRESSION FOR THE ELECTRON-PHONON HALF-WIDTH $\Gamma_{ep}(\vec{q}\lambda)$

As a natural starting point we observe that the electron-phonon collision operator for phonons is given by the Golden Rule (first-order perturbation theory) to be[31]

$$\left(\frac{\partial n(\omega_{q\lambda})}{\partial t}\right)_{\text{coll}} = \frac{-2\pi}{\hbar} 2 \sum_{kk'} \sum_{G} |M_\lambda(\vec{k}-\vec{k}')|^2 \Delta(\vec{k}'-\vec{k}+\vec{q}+\vec{G}) \times \delta(\epsilon_{k'}-\epsilon_k+\hbar\omega_{q\lambda}) \{f(\epsilon_{k'})[1-f(\epsilon_k)] n(\omega_{q\lambda}) - f(\epsilon_k)[1-f(\epsilon_{k'})][1+n(\omega_{q\lambda})]\} . \quad \text{(B1)}$$

The notation used here is fairly standard. $M_\lambda(\vec{k}-\vec{k}')$ is the matrix element (to be given later), $\vec{k}$ and $\vec{k}'$ are the wave vectors of the electrons, $\vec{G}$ is a reciprocal-lattice vector. The distribution functions for the electrons and phonons are, respectively, given by $f(\epsilon_k)$ and $n(\omega_{q\lambda})$. The sum over spin contributes the factor of 2 before the summation. The two terms in (B1) correspond to the processes depicted in Fig. 15.

Using Eq. (B1) we may now easily derive an expression for $\Gamma_{ep}(\vec{q}, \lambda)$. To do this we first observe that in equilibrium the collision operator is identically zero. If an additional phonon of wave vector $\vec{q}$ and polarization λ is then introduced into the system, i.e., for $n(\omega_{q\lambda}) \to n^{\text{equil}}(\omega_{q\lambda}) + \Delta n(\omega_{q\lambda})$, the collision integral becomes

$$\left(\frac{\partial}{\partial t}\Delta n(\omega_{q\lambda})\right)_{\text{coll}} = \frac{-4\pi}{\hbar} \sum_{kk'} \sum_{G} |M_\lambda(\vec{k}-\vec{k}')|^2 \times \Delta(k-k'+q+G)\, \delta(\epsilon_{k'}-\epsilon_k + \hbar\omega_{q\lambda})[f(\epsilon_{k'})-f(\epsilon_k)]\Delta n(\omega_{q\lambda}) . \quad \text{(B2)}$$

In this and all subsequent formulas $f(\epsilon_k)$ is understood to be the equilibrium distribution function, i.e., $f(\epsilon_k) = [e^{\epsilon_k/k_BT}+1]^{-1}$. Furthermore, in the relaxation-time approximation $1/\tau_{ep}(\vec{q}, \lambda)$ is defined by

$$\left(\frac{\partial}{\partial t}\Delta n(\omega_{q\lambda})\right)_{\text{coll}} \equiv \frac{-\Delta n(\omega_{q\lambda})}{\tau_{ep}(\vec{q}, \lambda)} . \quad \text{(B3)}$$

Furthermore we can identify our Golden-Rule calculation of $1/\tau_{ep}(\vec{q}, \lambda)$ with the imaginary part of the phonon self-energy due to the electron-phonon interaction $\Gamma_{ep}(\vec{q}\lambda)$ by the expression

$$\frac{1}{\tau_{ep}(q, \lambda)} = 2\Gamma_{ep}(\vec{q}, \lambda) . \quad \text{(B4)}$$

Compare, for example, our result for longitudinal, long-wavelength phonons (B8) with the same limit for the imaginary part of the self-energy derived by Kokkedee[32] [Eq. (5.11) of his paper]. Using (B2)–(B4) we then have

$$\frac{1}{\tau_{ep}(q, \lambda)} = 2\Gamma_{ep}(\vec{q}\lambda) = \frac{4\pi}{\hbar} \sum_{kk'} \sum_{G} |M_\lambda(\vec{k}-\vec{k}')|^2 \Delta(\vec{k}'-\vec{k}+\vec{q}+\vec{G}) \times \delta(\epsilon_{k'}+\hbar\omega_{q\lambda}-\epsilon_k)[f(\epsilon_{k'})-f(\epsilon_k)] . \quad \text{(B5)}$$

In the pseudopotential approximation for a simple metal like potassium the squared matrix element for scattering between plane-wave states $\vec{k}$ and $\vec{k}'$ is given by[33]

$$|M_\lambda(\vec{k}-\vec{k}')|^2 = \frac{\hbar}{2MN\omega_{k-k',\lambda}} |V(\vec{k}-\vec{k}')|^2 \times |(\vec{k}-\vec{k}')\cdot\hat{\epsilon}_{k-k',\lambda}|^2 , \quad \text{(B6)}$$

where $V|(\vec{k}-\vec{k}')|^2$ is the pseudopotential, M is the

TABLE V. Effect of the change in mesh size and the value used for ϵ on the phonon-phonon half-widths. Value of ϵ used for the 1024-point calculations was 6.5×10^{11} rad/sec (5 K in temperature units); for the 11 664-point mesh size $\epsilon = 1\times10^{11}$ rad/sec (1 K); and finally for the 54 000-point mesh size ϵ was set equal to 5×10^{10} rad/sec (0.5 K). All the half-widths were calculated for a temperature of 1 K.

Number of points in Brillouin zone	$\vec{q}$ ($2\pi/a$)	Γ_L^{tot}	$\Gamma_{T_h}^{\text{tot}}$	$\Gamma_{T_l}^{\text{tot}}$	Γ_L^U	$\Gamma_{T_h}^U = \Gamma_{T_l}^U$
		(10^8 rad/sec)			(10^8 rad/sec)	
1 024	(0.1, 0, 0)	5	1		0.2	0.5
11 664		1	0.2		0.04	0.009
			$T_h = T_l$			
1 024	(0.2, 0, 0)	20	5		2	0.6
11 664		10	1		0.3	0.09
			$T_h = T_l$			
1 024		2	0.5	1	...	...
11 664	(0.05, 0.05, 0)	0.4	0.1	0.2	...	...
54 000		0.2	0.05	0.1	...	...

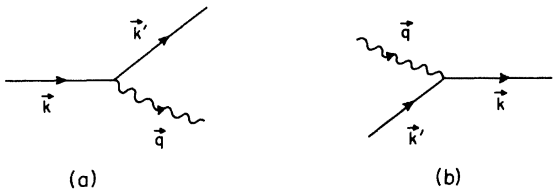

FIG. 15. Processes contribution to Γ_{ep}. (a) An electron with wave vector $\vec{k}$ scatters into a state with wave vector $\vec{k}'$ *emitting* a phonon of wave vector $\vec{q}$. (b) An electron with wave vector $\vec{k}'$ *absorbs* a phonon of wave vector $\vec{q}$ while scattering into a state with wave vector k. Process (a) tends to *increase* the phonon population $N(\omega_q)$ while process (b) tends to *decrease* $N(\omega_q)$.

ionic mass, and N is the number of cells per unit volume. In our calculations we have used the Ashcroft pseudopotential[34] for $V(|\vec{k}-\vec{k}'|)$ with $R_c = 1.13$ Å for potassium, $R_c = 1.27$ Å for rubidium, and $R_c = 0.59$ Å for aluminum[35] (see Fig. 16).

For a free-electron-like material which has a spherical Fermi surface that does *not* intersect the Brillouin-zone boundaries, such as is the case for potassium, the integrations in Eq. (B4) are straightforward. See Appendix C for the details. The final result is

$$\frac{1}{\tau_{ep}(q,\lambda)} = 2\Gamma_{ep}(\vec{q},\lambda) = \frac{m^2}{2\pi\rho\hbar^3}\sum_G |V(Q)|^2 \frac{|\vec{Q}\cdot\hat{\epsilon}_{q\lambda}|^2}{|\vec{Q}|}\Theta(2k_F - Q), \tag{B7}$$

where $\vec{Q} = \vec{q} + \vec{G}$, ρ is the ion mass density, and $\Theta(x)$ is the unit step function. In the long-wavelength limit ($q \to 0$) for longitudinal phonons, using $|\hat{q}\cdot\hat{\epsilon}_{qL}| \to 1$ and $V(Q) \to -\frac{2}{3}\epsilon_F$, we have the simple result that

$$2\Gamma_{ep}(\vec{q}, L) = \tfrac{1}{6}\pi(m/M)\, v_F q\,. \tag{B8}$$

We wish to thank Bill Buyers for his assistance in making the correct connection between our calculations for this rate and those of him and Cowley reported in Ref. 20.

APPENDIX C: INTEGRATIONS IN EQ. (B2) OF APPENDIX B

In particular we need to integrate the expression

$$I = \sum_{kk'} \frac{|V(\vec{k}-\vec{k}')|^2}{\omega_{k-k'\lambda}} |(\vec{k}-\vec{k}')\cdot\hat{\epsilon}_{k-k'\lambda}|^2 \Delta(\vec{k}'-\vec{k}+\vec{Q}) \times \delta(\epsilon_{k'} + \hbar\omega_{q\lambda} - \epsilon_k)[f(\epsilon_{k'}) - f(\epsilon_k)]\,. \tag{C1}$$

For a spherical Fermi surface that does not intersect the Brillouin-zone boundary it is useful to divide the integrals of k and k into the usual surface and energy integrals[36]

$$\sum_{kk'} \to \left(\frac{1}{8\pi^3}\right)^2 \int \frac{dS_k}{\hbar v_k}\frac{dS_{k'}}{\hbar v_{k'}} \int d\epsilon_k\, d\epsilon_{k'}\,.$$

The energy integrals then trivially give

$$\int d\epsilon_k \int d\epsilon_{k'}\, \delta(\epsilon_{k'} + \hbar\omega_{q\lambda} - \epsilon_k)[f(\epsilon_{k'}) - f(\epsilon_k)] = \int d\epsilon_k [f(\epsilon_k - \hbar\omega_{q\lambda}) - f(\epsilon_k)] = \hbar\omega_{q\lambda}\int d\epsilon_k \left(-\frac{\partial f}{\partial \epsilon}\right) = \hbar\omega_{q\lambda}\,. \tag{C2}$$

The remaining surface integrals over the two Fermi surfaces may be done as follows:

$$\int \frac{dS_k}{\hbar v_k}\int \frac{dS_{k'}}{\hbar v_{k'}} (2\pi)^3 \delta^3(k' - k + Q) = \frac{(2\pi)^3 k_F^4}{\hbar^2 v_F^2}\int d\Omega_k \int d\Omega_{k'}\, \delta^3(\vec{k}' - \vec{k} + \vec{Q}). \tag{C3}$$

In these integrals both $\vec{k}$ and $\vec{k}'$ have a magnitude equal to k_F. Observing that

$$\delta^3(\vec{k}' - \vec{k} + \vec{Q}) = \delta(|\vec{k}'| - |\vec{k} - \vec{Q}|)\,\delta(\Omega_{k'} - \Omega_{\vec{k}-\vec{Q}})/k_F^2 = \delta(k_F - |\vec{k} - \vec{Q}|)\,\delta(\Omega_{k'} - \Omega_{\vec{k}-\vec{Q}})/k_F^2. \tag{C4}$$

Equation (C3) becomes after a trivial integration over $\Omega_{k'}$

$$\frac{(2\pi)^3 k_F^2}{\hbar^2 v_F^2}\int d(\cos\theta)\, d\varphi\, \delta(k_F - (k_F^2 + Q^2 - 2k_F Q\cos\theta)^{1/2}) = \frac{(2\pi)^3 k_F^2}{\hbar^2 v_F^2}\frac{2\pi}{Q}\Theta(2k_F - |\vec{Q}|). \tag{C5}$$

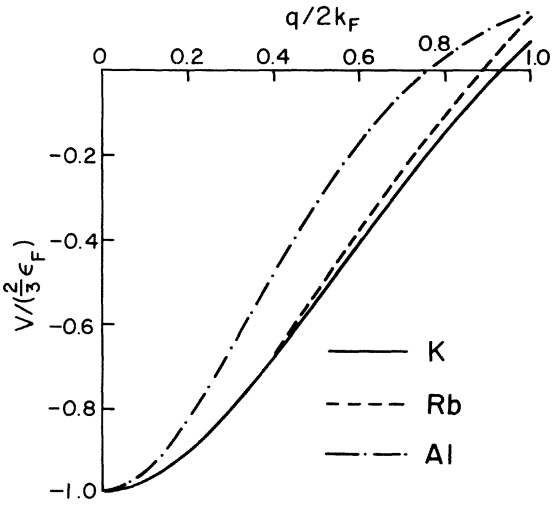

FIG. 16. Plot of the pseudopotentials that were used in the calculations of the electron-phonon half-widths for potassium, rubidium, and aluminum. They are all Ashcroft pseudopotentials with $R_c = 1.13$ Å for potassium, $R_c = 1.27$ Å for rubidium, and $R_c = 0.59$ Å for aluminum.

*Work supported in part by the National Science Foundation through Grant No. GH-36457, and by the National Science Foundation Grant No. GH-33637, through the Cornell Materials Science Center, MSC Report No. 2311.

†Present address: Konstruktions Material II, Chalmers Tekniska Högskola, 402 20 Göteborg, Sweden.

‡Also to be found at the Laboratory of Atomic and Solid State Physics and the Materials Science Center, Cornell University.

[1]R. E. Peierls, *Quantum Theory of Solids* (Oxford U. P. Oxford, England, 1955), p. 138.

[2]For asymptotic limits of the temperature dependence of Γ_{pp}, see Conyers Herring, Phys. Rev. 95, 954 (1954); and V. N. Kashcheev and M. A. Krivoglaz, Fiz. Tverd. Tela 13, 1528 (1961) [Sov. Phys.-Solid State 3, 1107 (1961)]. Γ_{ep} is calculated in Appendix B, where it is explicitly shown to be independent of temperature.

[3]F. Bloch, Z. Phys. 59, 208 (1930).

[4]The details of the resistivity calculation may be found in M. Roy, thesis (Cornell University, 1972) (unpublished); and M. Roy, Proceedings of Nuclear Physics and Solid State Physics Symposium, Indian Institute of Science, Bangalore C 16, 43 1973. We will publish further details of this work later when we are able to incorporate the phonon scattering rates into the calculation. For support of our Fig. 1 we refer the reader to the similar result of C. R. Leavens and M. J. Laubitz, J. Phys. F 5, 1519 (1975). Note the nature of the "switch" region is at variance with the conventional view.

[5]M. Roy, Pramana 2, 273 (1974)

[6](a) R. A. Cowley, A. D. B. Woods, and G. Dolling, Phys. Rev. 150, 487 (1966); (b) W. J. L. Buyers and R. A. Cowley, Phys. Rev. 180, 755 (1969); (c) M. S. Duesbery, Roger Taylor, and H. R. Glyde, Phys. Rev. B 8, 1372 (1973).

[7]J. R. D. Copley and B. N. Brockhouse, Can. J. Phys. 51, 657 (1973).

[8]J. R. D. Copley, Can. J. Phys. 51, 2564 (1973).

[9]T. Högberg and R. Sandström, Phys. Status Solidi 33, 169 (1969).

[10]T. R. Koehler, N. S. Gillis, and Duane C. Wallace, Phys. Rev. B 1, 4521 (1970).

[11]E. W. Prohofsky and J. A. Krumhansl, Phys. Rev. 133, A1403 (1964).

[12]See the review article of H. Beck, P. F. Merer, and A. Thellung, Phys. Status Solidi (to be published).

[13]Göran Niklasson, Phys. Kondens. Mater. 14, 138 (1972).

[14]See, for example, the article by Jules de Launay (Ref. 15). For further discussion of the relationship between the polarization vectors and the anisotropy index in metals see G. Grimvall, Phys. Status Solidi 32, 383 (1969). For a discussion and calculation of the polarization vectors of another metal, sodium, see G. B. Björkman and G. Grimvall, Phys. Status Solidi 19, 863 (1967).

[15]We have taken the values of the elastic constants from Table V of the article by Jules de Launay, in *Solid State Physics*, edited by H. Ehrenreich, F. Seitz, D. Turnbull (Academic, New York, 1956), Vol 2, p. 268.

[16]We have used $c_{11}=0.0416$, $c_{12}=0.0341$, $c_{44}=0.0286$ in units of 10^{12} dyn/cm^2; C. Kittel, *Introduction to Solid State Physics*, 4th ed. (Wiley, New York, 1971), p. 149 (values for 4 K).

[17]See, J. M. Ziman, *Electrons and Phonons* (Clarendon, Oxford, England, 1960), p. 358.

[18]Compare, for example, Fig. 1 of Ref. 8 with Fig. 1 of Ref. 20.

[19]Reference 8. The author also lists $T=0$ K results which may be questionable because of the difficulties of low-temperature calculations (c.f., Appendix A). Although he cautiously disclaims his calculation as being "barely adequate to determine the widths" we have proceeded with our analysis on the assumption that the higher-temperature results are reasonably correct.

[20]W. J. L. Buyers and R. A. Cowley, Phys. Rev. 180, 755 (1969).

[21]A. A. Maradudin and A. E. Fein, Phys. Rev. 128, 2600 (1962).

[22]S was calculated from the elastic constant measured by E. J. Gutman and J. Trivisonno, J. Phys. Chem. Solids 28, 805 (1967). The particular values used were extrapolated down to 4.2 K from data above 78 K.

[23]See, for example, (a) G. Björkman, B. I. Lundqvist, and A. Sjölander, Phys. Rev. 159, 551 (1967); and (b) T. Högberg and R. Sandström, Phys. Status Solidi 33, 169 (1969).

[24]R. Stedman and G. Nilsson, Phys. Rev. 145, 492 (1966).

[25]See, for example, L. Bohlin and T. Högberg, J. Phys. Chem. Solids 29, 1805 (1968).

[26]The details of the computer program are, with slight modification, those described in L. Bohlin, I. Ebbsjö, and T. Högberg, A. B. Atomenergi, Nyköping, Sweden, Report No. AE-348, 1969 (unpublished).

[27]In this case, E. R. Cowley has pointed out to us the work of V. V. Goldman, G. K. Horton, T. H. Keil, and M. L. Klein, J. Phys. C 3, L33 (1970), who use a Gilat-Raubenheimer method to handle the δ function without getting involved in the ϵ problem. If the phonons are treated as if they were sharp (i.e., having no width) in the calculation, then this method represents an advance over (A4). However, what is needed is an extension of the Gilat-Raubenheimer method which permits a logarithmic mesh with a Monte Carlo scheme which weights the low-q points.

[28]This was checked by looking at the oscillations in the ω dependence of Γ; c.f., Ref. 25.

[29]Reference 20. Their calculations, when converted to rad/sec, give $\Gamma_{pp}^{\rm tot}(L)=5\times10^{10}$ (at $\xi=0.2\times2\pi/a$) and 1.3×10^{11} rad/sec (at $\xi=0.4\times2\pi/a$) and $\Gamma_{pp}^{\rm tot}(T_h)=5\times10^{10}$ (at $\xi=0.2$) and 9×10^{10} rad/sec (at $\xi=0.4$).

[30]These numbers (listed in Table V) are the only calculations done using the 54 000-point mesh size.

[31]See, for example, Eq. (5-64) of David Pines, *Elementary Excitations in Solids* (Benjamin, New York, 1964), p. 260.

[32]J. J. J. Kokkedee, Physica (Utr.) 28, 893 (1962).

[33]For a discussion of the matrix element, see J. M. Ziman, *Electrons and Phonons* (Clarendon, Oxford, England, 1960), Chap. V. For a review of pseudopotential theory see the article by Volker Heine, Solid State Phys. 24, 1 (1970). As an example where the matrix element is written in a form almost identical to Eq. (B5), see B. Hayman and J. P. Carbotte, Can. J. Phys. 51, 1109 (1973).

[34]N. W. Ashcroft, Phys. Lett. 23, 48 (1966).

[35]For the core radius R_c of potassium and aluminum we

have used the value suggested by Ashcroft (Ref. 34). For the R_c of rubidium we have used the value suggested by J. R. D. Copley, Can. J. Phys. 51, 2569 (1973).

[36]See, for example, C. Kittel, *Introduction to Solid State Physics*, 4th ed. (Wiley, New York, 1971), pp. 210–211.